NeuroImage 273 (2023) 120097

Contents lists available at ScienceDirect

NeuroImage

journal homepage: www.elsevier.com/locate/neuroimage

Classical and non-classical psychedelic drugs induce common network changes in human cortex

Rui Dai[a,b,c,1], Tony E. Larkin[a,d,1], Zirui Huang[a,b,c], Vijay Tarnal[a,b,c], Paul Picton[a,b,c], Phillip E. Vlisides[a,b,c], Ellen Janke[a,b,c], Amy McKinney[a], Anthony G. Hudetz[a,b,c,e], Richard E. Harris[a,c,d,e], George A. Mashour[a,b,c,e,f,*]

[a] Department of Anesthesiology, University of Michigan Medical School, Ann Arbor, MI 48109, United States
[b] Center for Consciousness Science, University of Michigan Medical School, Ann Arbor, MI 48109, United States
[c] Michigan Psychedelic Center, University of Michigan Medical School, Ann Arbor, MI 48109, United States
[d] Chronic Pain and Fatigue Research Center, University of Michigan Medical School, Ann Arbor, MI 48109, United States
[e] Neuroscience Graduate Program, University of Michigan, Ann Arbor, MI 48109, United States
[f] Department of Pharmacology, University of Michigan Medical School, Ann Arbor, MI 48109, United States

ARTICLE INFO

Keywords:
Consciousness
Nitrous oxide
Ketamine
LSD
fMRI
Functional connectivity
Cortex

ABSTRACT

The neurobiology of the psychedelic experience is not fully understood. Identifying common brain network changes induced by both classical (i.e., acting at the 5-HT_2 receptor) and non-classical psychedelics would provide mechanistic insight into state-specific characteristics. We analyzed whole-brain functional connectivity based on resting-state fMRI data in humans, acquired before and during the administration of nitrous oxide, ketamine, and lysergic acid diethylamide. We report that, despite distinct molecular mechanisms and modes of delivery, all three psychedelics reduced within-network functional connectivity and enhanced between-network functional connectivity. More specifically, all three drugs increased connectivity between right temporoparietal junction and bilateral intraparietal sulcus as well as between precuneus and left intraparietal sulcus. These regions fall within the posterior cortical "hot zone," posited to mediate the qualitative aspects of experience. Thus, both classical and non-classical psychedelics modulate networks within an area of known relevance for consciousness, identifying a biologically plausible candidate for their subjective effects.

1. Introduction

The neurobiological basis of the psychedelic experience remains incompletely understood. One approach to deeper mechanistic insight would be the identification of drug-invariant neural correlates induced by diverse psychedelic drugs. Classical psychedelics such as lysergic acid diethylamide (LSD) are thought to exert their subjective effects primarily through the serotonergic 5-HT_2 receptor. There are related drugs such as ketamine, an NMDA receptor antagonist, which does not act primarily on 5-HT_2 receptors but, like classical psychedelics, induces similar phenomenology (Studerus et al., 2010), increases neurophysiologic complexity (Li and Mashour, 2019; Schartner et al., 2017), depresses posterior cortical alpha oscillations (Vlisides et al., 2018), expands the repertoire of functional brain connectivity states (Li et al., 2022), induces neuroplasticity (Phoumthipphavong et al., 2016), and has antidepressant effects (Berman et al., 2000). For the purpose of this article, we refer to drugs that induce similar effects through a primarily non-serotonergic mechanism as "non-classical" psychedelics.

Nitrous oxide is another NMDA receptor antagonist (Jevtović-Todorović et al., 1998) that has been in continuous clinical use as an anesthetic since the mid-19th century and that has psychedelic properties at subanesthetic concentrations (Block et al., 1990). Unlike LSD and ketamine, there is a paucity of data on the neural correlates of the psychedelic experience induced by nitrous oxide, despite longstanding use of this inhaled drug and a description of its psychological effects by William James more than a century ago (James, 1874). Various electroencephalographic and magnetoencephalographic studies in humans have reported spectral, functional connectivity, and complexity changes associated with nitrous oxide (Foster and Liley, 2013; John et al., 2001; Pavone et al., 2016; Pelentritou et al., 2020; Ryu et al., 2017; Vrijdag et al., 2021), but at sedative rather than psychedelic concentrations, or without assessment of psychedelic phenomenology. Although

* Corresponding authors at: Department of Anesthesiology, 1301 Catherine Street, 4102 Medical-Science Building 1, Ann Arbor, MI 48109, United States
E-mail addresses: reharris@med.umich.edu (R.E. Harris), gmashour@med.umich.edu (G.A. Mashour).
[1] These authors contributed equally to this work.

https://doi.org/10.1016/j.neuroimage.2023.120097.
Received 22 October 2022; Received in revised form 6 March 2023; Accepted 6 April 2023
Available online 7 April 2023.

there has been investigation of the effect of nitrous oxide on cerebral blood flow using magnetic resonance imaging (MRI) (Dashdorj et al., 2013), there have been no functional MRI (fMRI) studies during nitrous oxide exposure in humans that have characterized changes in functional brain networks associated with psychedelic effects. Thus, the neural correlates of the psychedelic experience induced by nitrous oxide, and the relationship of such correlates to the neurobiology of other psychoactive drugs such as LSD or ketamine, is unclear.

We conducted a neuroimaging study of healthy human volunteers, who were assessed with a validated altered states questionnaire before and after exposure to psychedelic concentrations of nitrous oxide. We analyzed whole-brain functional connectivity based on MRI data acquired before and during the administration of nitrous oxide. To compare the neural correlates of the psychedelic experience induced by nitrous oxide to other drugs, we conducted a secondary analysis of fMRI data acquired during exposure to subanesthetic ketamine and LSD. To control for generic changes in connectivity that might occur during non-psychedelic state transitions, we conducted a secondary analysis of fMRI data acquired during sedation with propofol, an anesthetic that acts as a $GABA_A$ receptor agonist (Hemmings et al., 2019).

2. Materials and methods

2.1. Dataset 1: nitrous oxide

This study was conducted at the University of Michigan Medical School, where Institutional Review Board (IRB, HUM00096321) approval was obtained. The study team carefully discussed risks and benefits with all participants, after which written informed consent was documented. This analysis was part of a clinical study registered with clinicaltrials.gov (NCT03435055); results from the primary study were posted in July 2021.

Except for two subjects' data that were completely discarded due to excessive head motion (50% of tagged fMRI volumes), a total of 16 participants (8 females, means ± SD, ages: 24.6 ± 3.7 years) completed two fMRI resting-state scans before and during exposure to subanesthetic concentrations (35%) of nitrous oxide. All participants were classified as American Society of Anesthesiologists physical status I, i.e., healthy. Drug abuse and history of psychosis were exclusion criteria, among other health-related conditions (see published registry for details: https://www.clinicaltrials.gov/ct2/show/NCT03435055).

We applied a within-subject design for both fMRI and altered states assessment. Each volunteer participated in two study visits, an initial consent/pre-scan visit and then a scanning visit within three days. During the pre-scan visit, participants were consented and presented with the details of the study protocol and what they would experience during the scanning session. During the scanning visit, each participant first completed a validated altered-states-of-consciousness questionnaire (Studerus et al., 2010), used for characterizing specific experiences rather than general state profiling. Participants were asked to complete the survey based on experiences during the two weeks that had just passed. Thereafter, fMRI data were collected during placebo (pure oxygen, 20 min) followed by inhaled nitrous oxide at subanesthetic concentrations (35%, in oxygen) over 40 min. It is standard clinical practice to administer 100% oxygen in advance of an inhaled anesthetic because it allows the lungs to denitrogenate and enhances oxygen reserve in the event of sedation-related airway obstruction or compromise. The administration of nitrous oxide was initiated before entering the scanner to achieve at least 5 min of equilibrium prior to the start of the resting state scan so we could monitor and address any adverse physiological or psychological reactions to the state transition. Pressure and visual stimuli, related to a protocol assessing analgesic effects (data not presented here), were not presented until after the resting state scan, to acquire the cleanest data possible. Only resting state fMRI data were analyzed for the purpose of this study. After scanning and 30 min of recovery from nitrous oxide administration, the altered states questionnaire was administered again. Participants were asked to complete the survey based on the study period during which nitrous oxide was administered. Among these 16 participants, 13 produced complete data from the altered states questionnaire, whereas three did not complete the questionnaire.

To maximize safety, nitrous oxide was delivered using MRI-compatible anesthesia machines, and was first administered outside of the scanner, where airway patency and physiological stability were established prior to imaging. At least two fully trained anesthesiologists directed all anesthetic administration. All participants received ondansetron (4–8 mg IV) with an additional dose of dexamethasone (4 mg IV) if needed to prevent nausea and vomiting. In addition, glycoyrrolate (0.42–0.4 mg IV), labetalol (5–10 mg/kg IV), and midazolam (1–2 mg IV) were available to mitigate any side effects. Standard intraoperative monitors (electrocardiogram, blood pressure, pulse oximetry, capnography) were used throughout the experiment. Participants wore earplugs and headphones during the fMRI scanning.

Data were acquired at Michigan Medicine, University of Michigan, using a Philips Achieva 3T scanner (Best, Netherlands). Functional images of the whole brain were acquired by a $T2^*$ weighted echo-planar sequence with parameters: 48 slices, TR/TE = 2000/30 ms, slice thickness = 3 mm, field of view = 200 × 200 mm, flip angle = 90°, scan time = 6 min. High-resolution anatomical images were also acquired for resting state fMRI co-registration.

2.2. Dataset 2: ketamine

This dataset has been previously published based on hypotheses and analyses that were distinct from those of the current study (Huang et al., 2020). The investigation was approved by the IRB of Huashan Hospital, Fudan University; informed consent was obtained from all participants. Twelve right-handed participants were recruited (5 females, means ± SD, ages: 41.4 ± 8.6 years). The volunteers were American Society of Anesthesiologists physical status I or II, with no history of brain dysfunction, major organ dysfunction, or use of neuropsychiatric drugs.

Ketamine was infused through an intravenous catheter placed into a vein of the left forearm. fMRI scanning was conducted throughout the whole experiment, ranging from 44 to 62 min (means ± SD, 54.6 ± 5.9 min). A 10 min baseline conscious condition was first acquired (except for two participants for whom baseline condition was 6 and 11 min). Then, 0.05 mg/ kg per minute of ketamine was infused for 10 min (0.5 mg/kg in total), and 0.1 mg/kg per minute was infused for another 10 min (1.0 mg/kg in total), except for two participants who only received 0.1 mg/kg per minute infusion for 10 min. The ketamine infusion was then discontinued and participants regained responsiveness spontaneously. Two certified anesthesiologists were present throughout the study, with resuscitation equipment always available. Participants wore earplugs and headphones during the fMRI scanning. The complete protocol includes (1) the period before ketamine-induced loss of responsiveness, and (2) the period during ketamine-induced loss of responsiveness. Because our focus was psychedelic experiences that typically occur during exposure to subanesthetic concentrations, only the period before loss of responsiveness was analyzed.

A Siemens 3T scanner (Siemens MAGNETOM, Germany) with a standard eight-channel head coil was used. Functional images from the whole brain were acquired by a gradient-echo EPI pulse sequence with parameters: 33 slices, TR/TE = 2000/30 ms, slice thickness = 5 mm, field of view = 210 mm, image matrix = 64 × 64, flip angle = 90°, scan time = 12 min. High-resolution anatomical images were also acquired for resting state fMRI co-registration.

2.3. Dataset 3: LSD

These data were obtained from an open-access database (doi:10.18112/openneuro.ds003059.v1.0.0); data from 20 partici-

pants were collected. One participant did not complete BOLD scans due to anxiety and an expressed desire to exit the scanner, and four others were excluded from the group analyses due to excessive head movement. Thus, 15 participants (5 females, means ± SD, ages: 38.4 ± 8.6 y) were included in the online repository.

Drug abuse and history of psychosis were exclusion criteria, among other health-related conditions (see published article for details in (Carhart-Harris et al., 2016)). Volunteers received placebo and LSD across two sessions; the order was counterbalanced across participants. A cannula was inserted and secured in a vein in the antecubital fossa by a medical doctor. All participants received 75 μg of LSD, administered intravenously via a 10 ml solution infused over a 2 min period, followed by an infusion of saline. MRI scanning started approximately 70 min after dosing, to capture changes associated with peak intensity between 60 and 90 min after administration.

Imaging was performed on a 3T GE HDx system. Functional images across the whole brain were acquired by a gradient-echo EPI pulse sequence with parameters: 35 slices, TR/TE = 2000/35 ms, slice thickness = 3.4 mm, field of view = 220 mm, image matrix = 64 × 64, flip angle = 90°, scan time = 7 min. High-resolution anatomical images were also acquired for resting state fMRI co-registration.

2.4. Dataset 4: propofol

Propofol is a sedative-hypnotic drug that is used for the induction and maintenance of anesthesia or sedation. We used propofol as a control for general brain state transitions that are not related to the psychedelic experience. The propofol dataset has been previously published using analyses distinct from those applied here (Huang et al., 2020, 2018b, 2016). The study was approved by the IRB of Huashan Hospital, Fudan University. Informed consent was obtained from all participants (n = 26; right-handed). Inclusion criteria, anesthetic procedures, fMRI details, scanning parameters, and clinical monitoring were the same as those described for ketamine. Only the data during the sub-anesthetic dosing (associated with light sedation; n = 17, 10 females, means ± SD, ages: 41.4 ± 8.6 years) were analyzed in the current study.

Propofol was infused through an intravenous catheter placed in a vein of the right hand or forearm. Propofol was administered using a target-controlled infusion pump to obtain and maintain consistent effect-site concentrations, as estimated by the pharmacokinetic model of propofol (Marsh model). TCI concentrations were increased in 0.1 μg/ml steps beginning at 1.0 μg/ml until reaching the appropriate effect-site concentration. A 5 min equilibration period was allowed to ensure equilibration of propofol distribution between compartments. The target-controlled propofol infusion was maintained at a stable effect-site concentration for light sedation (1.3 μg/ml). The participants continued to breathe spontaneously with supplemental oxygen via nasal cannula.

A Siemens 3T scanner (Siemens MAGNETOM, Germany) with a standard eight-channel head coil was used. Functional images across the whole brain were acquired by a gradient-echo EPI pulse sequence with parameters: 33 slices, TR/TE = 2000/30 ms, slice thickness = 5 mm, field of view = 210 mm, image matrix = 64 × 64, flip angle = 90°, scan time = 8 min. High-resolution anatomical images were also acquired for resting state fMRI co-registration.

2.5. Altered states questionnaire

The altered-states-of-consciousness questionnaire is composed of 11 dimensions, including the following: experiences of unity, spiritual experience, blissful state, insightfulness, disembodiment, impaired control and cognition, anxiety, complex imagery, elementary imagery, audiovisual synesthesia, and changed meaning of percepts. For all items, the response scale was from 0 (Never) to 10 (Always) with 11 total discrete response options. Scale scores reported here were the average of items within each scale.

2.6. fMRI data preprocessing

Preprocessing steps were implemented in the CONN toolbox (https://web.conn-toolbox.org/) and included: (1) slice timing correction; (2) rigid head motion correction/realignment within and across runs. Frame-wise displacement (FD) of head motion was calculated using frame-wise Euclidean Norm (square root of the sum squares) of the six-dimension motion derivatives. A given frame and its previous frame were tagged as zeros if the frame's derivative value had a Euclidean Norm above FD = 0.9 mm or the BOLD signal changed above 5 SD (otherwise it was tagged as ones); (3) co-registration with high-resolution anatomical images; (4) spatial normalization into MNI (Montreal Neurological Institute) space and resampling to 3 × 3 × 3 mm^3; (5) time-censored data were low- and high-pass filtered (>0.008, <0.09 Hz). At the same time, various undesired components were removed via linear regression. The undesired components included linear and nonlinear drift, time series of head motion and its temporal derivative, and mean time series from the white matter and cerebrospinal fluid; 6) spatial smoothing with 6 mm full-width at half-maximum isotropic Gaussian kernel. After preprocessing and denoising, the data were visually examined for quality assurance.

Dataset 3 has been preprocessed and published (doi:10.18112/openneuro.ds003059.v1.0.0). The data preprocessing steps included: (1) removal of the first three volumes; (2) de-spiking; (3) slice time correction; (4) motion correction; (5) brain extraction; (6) rigid body registration to anatomical scans; (7) non-linear registration to 2 mm MNI brain; (8) scrubbing (Power et al., 2012), using an FD threshold of 0.4. The maximum number of scrubbed volumes per scan was 7.1% and scrubbed volumes were replaced with the mean of the surrounding volumes. Additional pre-processing steps included: (9) spatial smoothing of 6 mm; (10) band-pass filtering between 0.01 and 0.08 Hz; (11) linear and quadratic de-trending; (12) regressing out undesired components (e.g., motion-related and anatomically related parameters).

In dataset 1, the mean percentage of volumes (means ± SD), scrubbed for baseline and nitrous oxide periods was 3.9 ± 6.3% and 6.1 ± 4.5%, respectively. Two subjects' data were completely discarded due to an excessive 50% of tagged volumes. In dataset 2, the mean percentage of volumes scrubbed for baseline and ketamine was 0.08 ± 0.2% and 0.3 ± 1%, respectively. No datasets were completely discarded due to an excessive number of tagged volumes. In dataset 3, the mean percentage of volumes scrubbed for baseline and LSD was 0.4 ± 0.8% and 1.7 ± 2.3%, respectively. No datasets were completely discarded due to an excessive number of tagged volumes. In dataset 4, the mean percentage of volumes scrubbed for baseline and propofol was 0.7 ± 1.5% and 6.8 ± 13.9%, respectively. No datasets were completely discarded due to an excessive number of tagged volumes. Except for the LSD data, we performed a paired t-test of FD between baseline and drug exposure for each drug; non-significant results were found (nitrous oxide: p = 0.15, ketamine: p = 0.43, propofol=0.097).

The majority of processing steps used in our primary datasets (nitrous oxide, ketamine, propofol) and that of the publicly available LSD dataset were the same. The main difference pertains to the FD threshold, which we optimized for the nitrous oxide data. In our nitrous oxide dataset, FD=0.9 mm preserved at least 150 fMRI frames (5 min) of continuous data across all subjects. In order to maintain consistency across different datasets, FD=0.9 mm was applied to ketamine and propofol datasets. To further examine if the choice of FD threshold would affect our main results, we applied FD=0.4 to the nitrous oxide, ketamine, and propofol data. The preserved data included 50% of subjects (8/16) with >66.70% continuous data (4 min/6 min) for nitrous oxide, 100% of subjects (12/12) with >66.7% continuous data (6.7 min/10 min) for ketamine, and 88% of subjects (15/17) with >66.7% continuous data (5.3 min/8 min) for propofol. Resting-state functional connectivity analyses were performed again. Due to a reduced number of time points and sample size, the significant results were sparser. However, the results of FD=0.4 (Fig. S1) were similar to those of FD=0.9.

2.7. Analysis of ROI-to-ROI functional connectivity

Region-of-interest (ROI)-to-ROI functional connectivity analysis was performed using the CONN toolbox (https://web.conn-toolbox.org/). The acquired functional connectivity matrices characterized the connectivity between all pairs of ROIs among a default CONN network parcellation from independent component analysis of the human connectome project (HCP) dataset (n = 497). This HCP-ICA atlas (Whitfield-Gabrieli and Nieto-Castanon, 2012) covered the main functions of the whole brain, which is divided into seven cerebral networks (default mode network, dorsal attention network, frontoparietal network, language network, salience network, sensorimotor network, visual network) plus one cerebellar network and their corresponding 32 ROIs (Table S1). Each element in the matrix indicates a Fisher-transformed bivariate correlation coefficient between a pair of ROI time courses.

2.8. Analysis of seed-based functional connectivity

Seed-based functional connectivity maps were computed as the Fisher-transformed bivariate correlation coefficients between the seed BOLD timeseries and each individual voxel BOLD timeseries. Random Field Theory parametric statistics were performed to control for family-wise error at the level of individual clusters (Chumbley et al., 2010). The right temporoparietal junction (TPJ) ROI was defined based on classical literature (Mars et al., 2012). This region was a focus because of its association with psychedelic drug administration in this study, and because it is thought to be critical to multisensory integration, consciousness, and body ownership (Arzy et al., 2006; Vlisides et al., 2018).

2.9. Statistical analysis

For the altered states questionnaire statistical analysis, we performed paired sample t-tests on the mean sub-scale scores between each psychedelic condition and baseline condition. After multiple comparisons, the statistical significance was set at FDR-corrected $p < 0.05$ (namely, pFDR < 0.05).

For ROI-to-ROI functional connectivity, we used standard settings for cluster-based inferences through functional network connectivity parametric multivariate statistics (Jafri et al., 2008) (i.e., CONN's standard settings for cluster-based inferences). The functional network connectivity metric analyzes the entire set of connections between all pairs of ROIs in terms of intra- and inter-network connectivity sets. We performed multivariate, parametric, general linear model analysis for all connections included in each of these sets/clusters of connections. As a final step for the obtained F-statistic for each pair of networks, a $p < 0.05$ was used together with an associated uncorrected cluster-level height and an FDR-corrected cluster-level threshold of $p < 0.05$, which controls the FDR. The FDR-controlling process provides less stringent control of Type I errors compared to family-wise error rate controlling procedures but has greater power (Shaffer, 1995). Due to the differences in scanner parameters between different psychedelic datasets, only within-group statistics were performed, i.e., each psychedelic condition was compared to its own baseline control condition rather than comparisons across different drugs.

In the analysis of seed-based functional connectivity, standard cluster-level inferences based on Gaussian Random Field theory (Worsley et al., 1996) were used. We performed paired sample t-tests on TPJ to whole-brain correlation maps for each psychedelic condition and its control condition; the statistical significance was set at pFDR < 0.05. To assess the degree of change in functional connectivity with the subjective degree of intensity of the psychedelic state induced by nitrous oxide, Spearman correlations were computed between seed-based functional connectivity changes (nitrous oxide versus its own baseline) and altered-states-of-consciousness score changes (nitrous oxide versus pre-nitrous oxide baseline); statistical significance was set at pFDR < 0.05. Statistics were computed with JASP (v0.16.3; https://jasp-stats.org/).

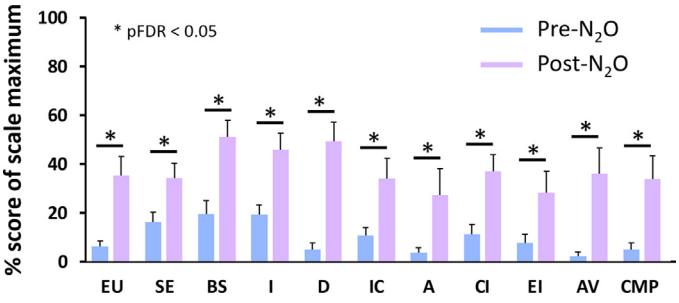

Fig. 1. Behavioral results derived from the 11D-altered states questionnaire. Error bars represent standard errors. EU: experience of unity, SE: spiritual experience, BS: blissful state, I: insightfulness, D: disembodiment, IC: impaired control and cognition, A: anxiety, CI: complex imagery, EI: elementary imagery, AV: audiovisua synesthesia, CMP: changed meaning of percepts. N_2O: nitrous oxide.

3. Results

3.1. Nitrous oxide as a psychedelic

Psychedelic experiences induced by LSD and ketamine have already been well described (Liechti et al., 2017; Studerus et al., 2010). To characterize altered state of consciousness induced by 35% nitrous oxide, the 11-D altered-states-of-consciousness questionnaire was performed. Nitrous oxide induced a significant change in each dimension when comparing study score to the pre-nitrous-oxide baseline score: experiences of unity (t (12) = 3.315, pFDR = 0.013), spiritual experience (t (12) = 2.855, pFDR = 0.017), blissful state ((t (12) = 3.692, pFDR = 0.011), insightfulness ((t (12) = 3.487, pFDR = 0.011), disembodiment ((t (12) = 5.302, pFDR = 0.002), impaired control and cognition ((t (12) = 3.066, pFDR = 0.015), anxiety ((t (12) = 2.237, pFDR = 0.045), complex imagery ((t (12) = 3.800, pFDR = 0.011), elementary imagery ((t (12) = 2.375, pFDR = 0.039), audiovisual synesthesia ((t (12) = 3.168, pFDR = 0.015), and changed meaning of percepts ((t (12) = 3.017, pFDR = 0.015). Overall, the altered-states-of-consciousness scores during nitrous oxide administration were higher than pre-nitrous oxide baseline scores on every subscale (Fig. 1). Among these 11 dimensions, the change in disembodiment was the most significant, consistent with the designation of nitrous oxide as a dissociative drug.

3.2. Effects of nitrous oxide on functional connectivity

Whole-brain ROI-to-ROI functional connectivity during the administration of nitrous oxide was analyzed in comparison with the control condition. Nitrous oxide increased connectivity *between* networks, including visual - salience network (pFDR = 0.007), dorsal attention – frontoparietal network (pFDR = 0.025), sensorimotor - language network (pFDR = 0.025), dorsal attention - language network (pFDR = 0.025), salience - default mode network (pFDR = 0.025), and dorsal attention – default mode network (pFDR = 0.025). Nitrous oxide decreased connectivity *within* salience network (pFDR = 0.025) and language network (pFDR = 0.025) (Fig. 2; see Fig. S2 for unthresholded metrics). Detailed statistics are reported in Table S2.

3.3. Effects of ketamine and LSD on functional connectivity

To compare the cortical network changes induced by nitrous oxide to those of other non-classical and classical psychedelic drugs, we analyzed ROI-to-ROI functional connectivity of the whole brain during exposure to psychedelic doses of ketamine and LSD using a within-group design. Compared to its own baseline, ketamine infusion enhanced between-network connectivity in frontoparietal - default mode network

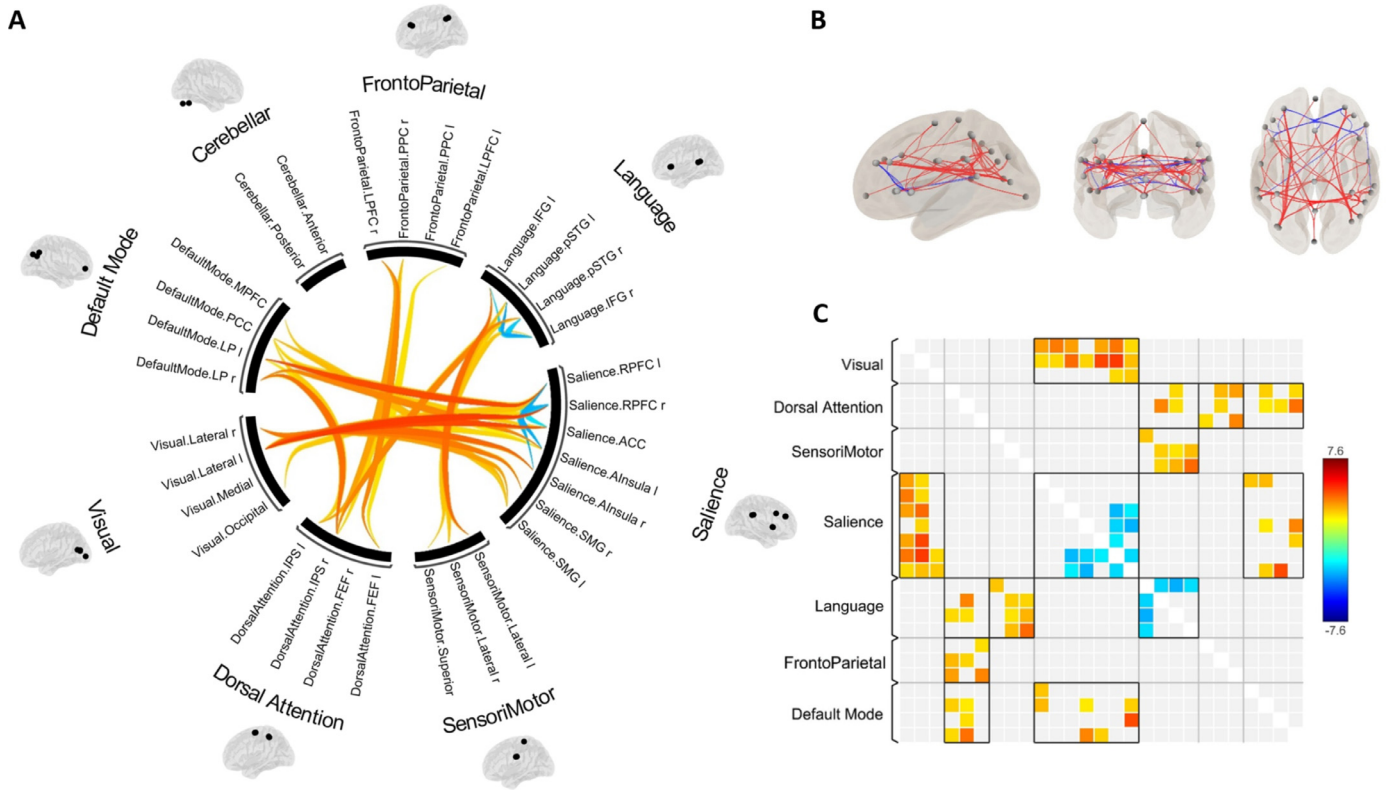

Fig. 2. Effects of nitrous oxide on functional connectivity. (A) The circle view displays significant functional connectivity changes (nitrous oxide versus control condition) between ROIs of seven cerebral cortical networks and one cerebellar network. (B) The connectome view displays the ROIs with individual suprathreshold connectivity lines between them. (C) Depiction of the ROI-to-ROI connectivity matrix of nitrous oxide versus control condition. Only significant ROI pairs are shown in the matrix.

(pFDR = 0.020), salience - default mode network (pFDR = 0.028), language - default mode network (pFDR = 0.031), dorsal attention - default mode network (pFDR = 0.045). Ketamine reduced within-network connectivity in frontoparietal network (pFDR = 0.020) and sensorimotor network (pFDR = 0.027) (Figs. 3. A-C; S2). Compared to its own baseline (Figs. 3. D-E; S2), LSD increased between-network connectivity in visual - language network (pFDR = 0.003), dorsal attention – language network (pFDR = 0.020), language - default mode network (pFDR = 0.020), visual - default mode network (pFDR = 0.025), dorsal attention – default mode network (pFDR = 0.025), salience - default mode network (pFDR = 0.035), sensorimotor - default mode network (pFDR = 0.042), and frontoparietal - default mode network (pFDR = 0.042). LSD decreased within-network connectivity in sensorimotor network (pFDR = 0.030) and dorsal attention network (pFDR = 0.030). Detailed statistics are reported in Tables S3 and S4.

Furthermore, we compared functional connectivity differences at the network level among the three psychedelic drugs, namely, nitrous oxide vs. ketamine, nitrous oxide vs. LSD, and ketamine vs. LSD. Although we observed some differences before FDR correction ($p < 0.05$, uncorrected), none of the networks showed significant differences after FDR correction (Fig. S3).

3.4. Common effects of psychedelics on functional connectivity

Based on network-level analyses, all three psychedelics decreased within-network connectivity and increased between-network connectivity (Fig. 4). However, functional connectivity changes between specific nodes differed according to the drug, as shown in the ROI-to-ROI analysis.

We further assessed whether there were common neural correlates of psychedelic drug administration at the ROI level. Four functional connectivity cluster pairs were consistently affected by all three psychedelics: right lateral parietal/ temporoparietal junction (TPJ) – left intraparietal sulcus, right lateral parietal – right intraparietal sulcus, precuneus cortex – left intraparietal sulcus and right lateral parietal – left anterior insula. These common changes occurred between networks. The first three pairs were between the default mode network and dorsal attention network, whereas the last pair was between the default mode network and salience network.

To confirm that these common connectivity patterns were not simply a generic feature of any pharmacologically altered state of consciousness, we analyzed fMRI data during baseline consciousness and propofol sedation as a control condition. Propofol is a clinical anesthetic that, at subanesthetic concentrations, alters consciousness without the typical features of the psychedelic experience. We performed the same whole-brain ROI-to-ROI functional connectivity analysis of the states before and during exposure to propofol sedation. As expected, unlike the psychedelic drugs there was no evidence of decreased within-network connectivity during subanesthetic propofol administration (Fig. S4 and Table S5), and only one functional connectivity cluster pair was consistent with the effect of the three psychedelics: right lateral parietal – left anterior insula (Fig. 5A). After eliminating the functional connectivity change also induced by subanesthetic propofol, three common cluster pairs were altered by psychedelic drug administration, including right TPJ/lateral parietal to bilateral IPS and precuneus to left IPS (Fig. 5B).

We conducted further analysis of the TPJ because of its association with psychedelic drug administration in this study, and because it is thought to be critical to multisensory integration, consciousness, body ownership, and the psychedelic effects of ketamine (Arzy et al., 2006; Vlisides et al., 2018). We performed a TPJ seed-based functional connectivity analysis in each group and compared the TPJ to the whole brain correlation map between each psychedelic condition and its control condition (Fig. 6). The overlap of the TPJ seed-based functional connectivity map across three psychedelics is in the bilateral IPS, which

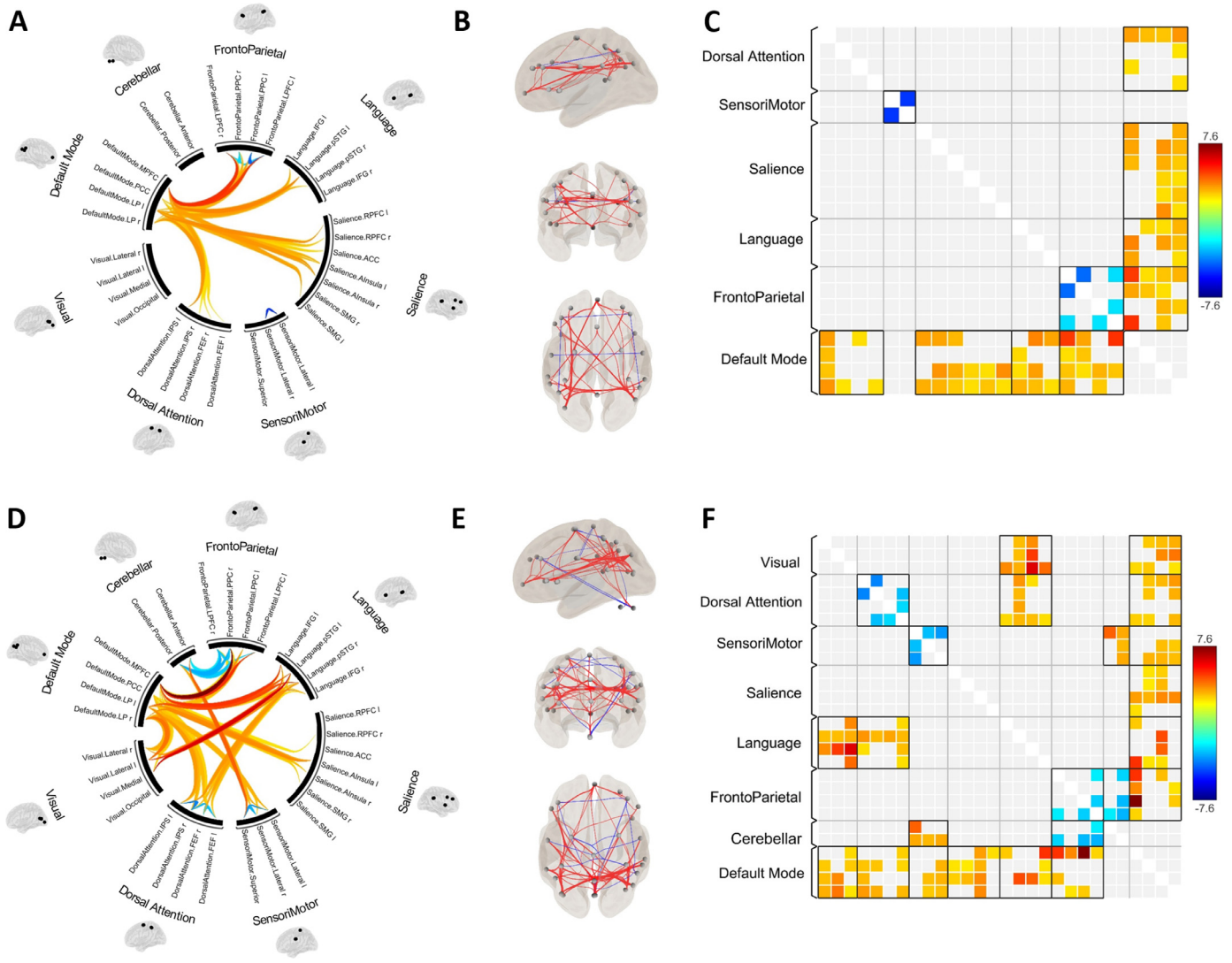

Fig. 3. Effects of psychedelic ketamine and LSD on functional connectivity. (A-C) circle view, connectome view, and correlation matrix of functional connectivity changes by ketamine relative to baseline. (D-E) circle view, connectome view, and correlation matrix of functional connectivity changes by LSD relative to baseline. Only significant ROI pairs are shown in the matrix.

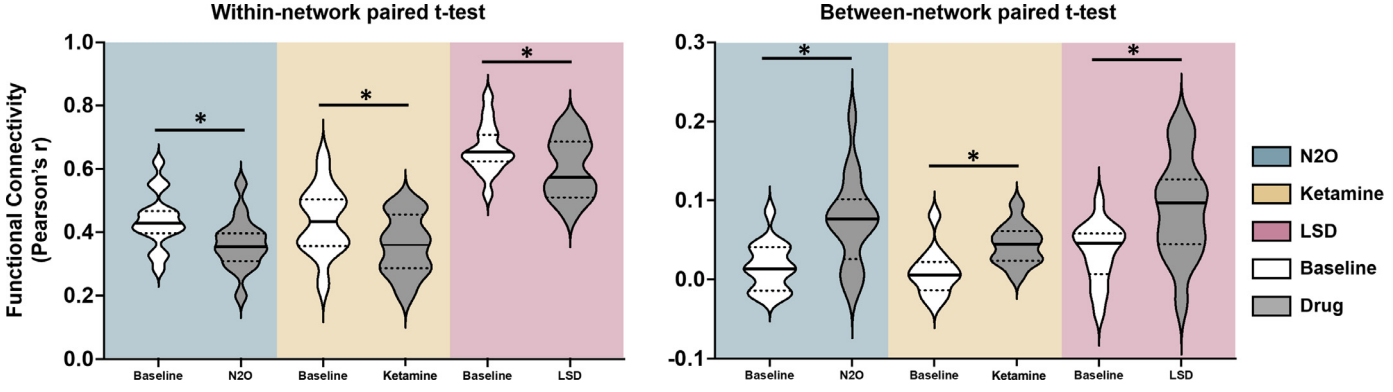

Fig. 4. Functional connectivity changes within and between networks. All three psychedelics significantly decreased within-network connectivity and increased between-network connectivity. $^{*}p < 0.05$, FDR corrected. N2O: nitrous oxide.

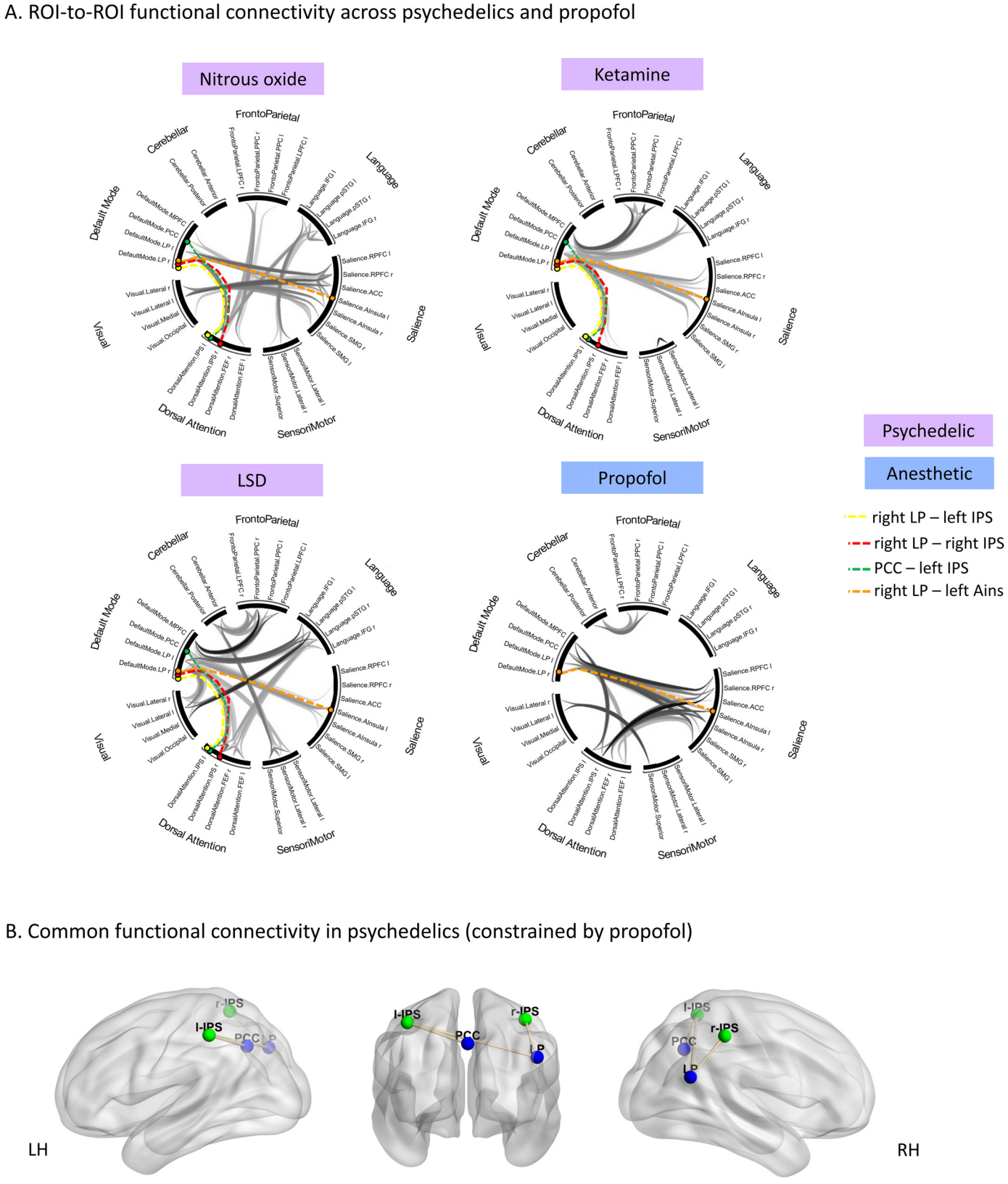

Fig. 5. Common effects of psychedelics on functional connectivity. (A) ROI-to-ROI functional connectivity changes induced by nitrous oxide, ketamine, LSD, and propofol. (B) Common functional connectivity patterns due to psychedelic drug administration after removing the change also induced by propofol sedation. LP: lateral parietal cortex, IPS: intraparietal sulcus, PCC: precuneus, Ains: anterior insula, LH: left hemisphere, RH: right hemisphere.

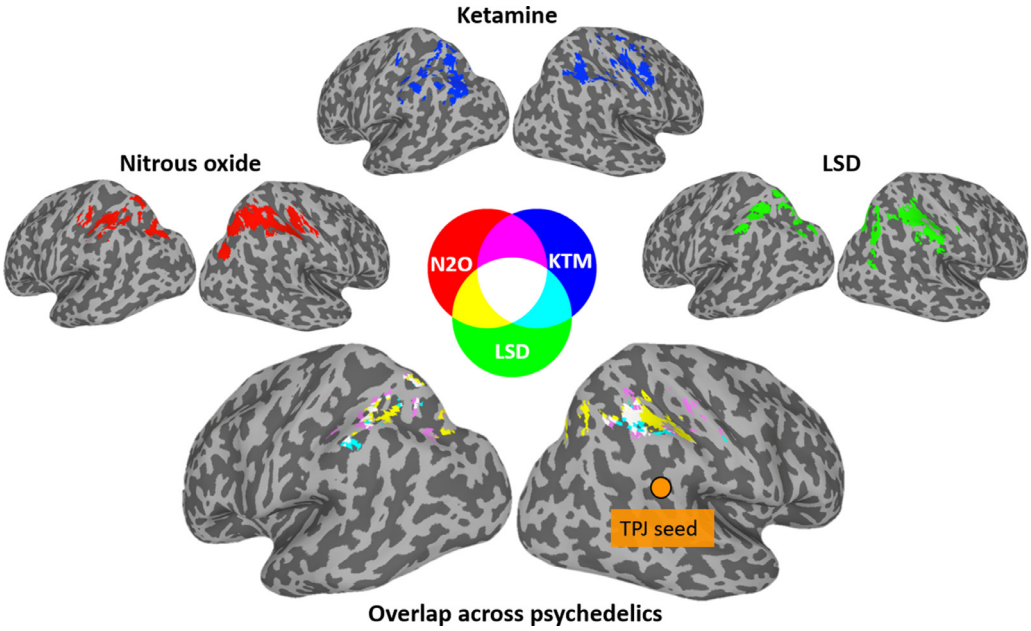

Fig. 6. Temporoparietal junction (TPJ) seed-based functional connectivity overlap with nitrous oxide, ketamine and LSD mapped onto an inflated cortical surface. Color code indicates the degree of consistency across the three psychedelics.

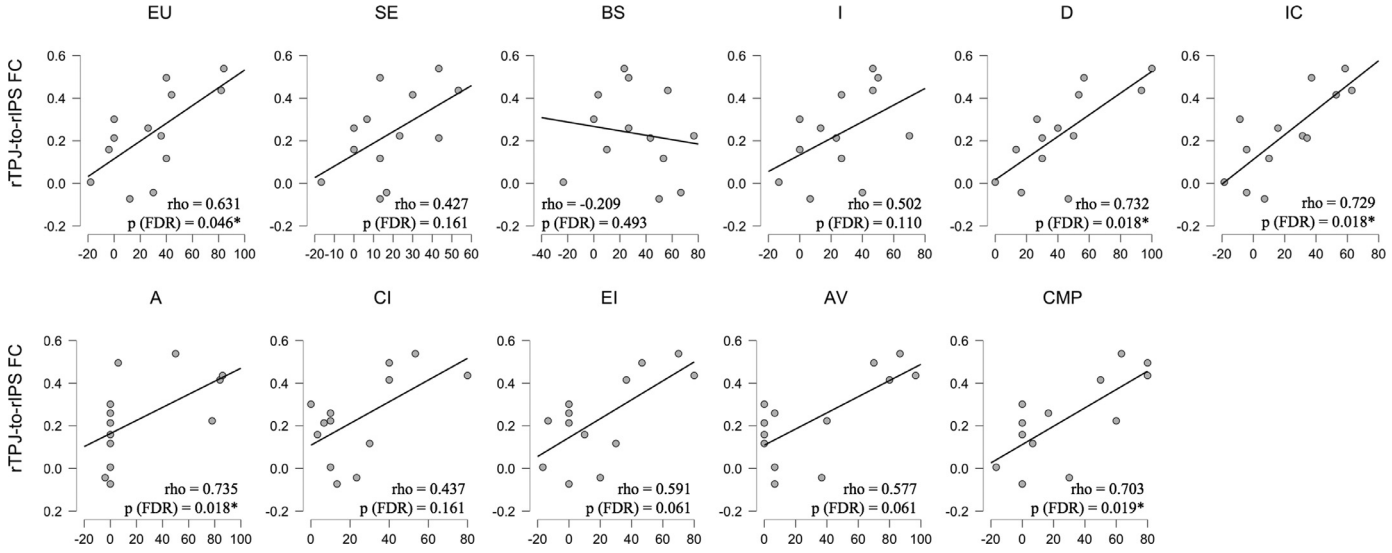

Fig. 7. Spearman correlations between right temporoparietal junction to right intraparietal sulcus functional connectivity changes (nitrous oxide versus its own baseline) and 11D-altered states questionnaire score changes (nitrous oxide versus pre-nitrous oxide baseline). Statistical significance was set at pFDR < 0.05. EU: experience of unity, SE: spiritual experience, BS: blissful state, I: insightfulness, D: disembodiment, IC: impaired control and cognition, A: anxiety, CI: complex imagery, EI: elementary imagery, AV: audiovisua synesthesia, CMP: changed meaning of percepts.

was expected because of the ROI-to-ROI functional connectivity results. In contrast, the TPJ seed-based functional connectivity result of propofol sedation is in the occipital cortex, non-overlapping with the functional connectivity patterns induced by nitrous oxide, ketamine, or LSD.

To explore the degree of change in TPJ-to-IPS functional connectivity with the subjective degree of intensity of the psychedelic state induced by nitrous oxide, we computed Spearman correlations between TPJ-to-IPS functional connectivity (nitrous oxide versus its own baseline) and altered-states-of-consciousness score changes (nitrous oxide versus its own baseline). We found that changes in TPJ to right IPS functional connectivity are significantly correlated with five subscales of 11D-altered states questionnaire, including disembodiment (pFDR = 0.018), impaired control and cognition (pFDR = 0.018), anxiety (pFDR = 0.018), changed meaning of percepts (pFDR = 0.019), and experience of unity (pFDR = 0.046) (Fig. 7 and Table S6).

4. Discussion

We demonstrate that non-classical (nitrous oxide, ketamine) and classical (LSD) psychedelic drugs all reduce within-network functional connectivity and increase between-network connectivity. Common neural correlates induced by these psychedelics, controlled for with the use of a non-psychedelic sedative-hypnotic, included increased connectivity between right TPJ and bilateral IPS and between precuneus and left IPS. These network nodes are located in the posterior cortical hot zone, which has been posited to be critical for content of consciousness, i.e., the qualitative aspects of our experience. The consistent results across non-classical and classical psychedelics support the hypothesis that there is a common neurobiology underlying the psychedelic effect at the level of large-scale brain networks. Furthermore, the posterior cortical confluence of sensory and association cortex is a biologi-

cally plausible candidate for the altered subjective experiences induced by psychedelic drugs. Finally, these data suggest the possibility that the psychedelic experience might not track with a single molecular mediator (e.g., $5HT_2$ receptor) but rather with network-level events that could have a diversity of molecular mechanisms. This is consistent with, for example, the common effects of ketamine and classical psychedelics on alpha oscillations, complexity, repertoire of brain states, neuroplasticity, and clinical effects (Berman et al., 2000; Li et al., 2022; Li and Mashour, 2019; Phoumthipphavong et al., 2016; Schartner et al., 2017; Studerus et al., 2010; Vlisides et al., 2018).

Specifically, TPJ was the region most consistently involved in psychedelic-induced connectivity changes from both ROI-to-ROI and seed-based functional connectivity analyses. It is known that TPJ is important for multisensory integration and body ownership (Arzy et al., 2006), modulation of which might contribute to psychedelic phenomenology (Vlisides et al., 2018). We controlled for the possibility that these changes might reflect a generic brain state transition through a comparison with propofol sedation, which induces functional connectivity changes opposite to those produced by psychedelics, namely, enhanced within-network connectivity and reduced between-network connectivity (Huang et al., 2018a). Through this control analysis, we were able to eliminate connectivity changes in anterior insula, which was common to all four drugs and thus likely unrelated to the psychedelic state.

The findings of our study inform not only psychedelic neuroscience but emerging psychedelic therapy. Nitrous oxide has been found to have anti-depressant effects in patients with treatment-resistant major depressive disorder (Nagele et al., 2015). More recently, it has been shown that a 25% concentration of nitrous oxide is as effective as a 50% concentration for treatment-resistant major depression (Nagele et al., 2021). The current study informs the network-level events in the brain that occur during exposure to a comparable concentration of nitrous oxide. Furthermore, ketamine, LSD, and other psychedelics have shown promise as anti-depressants (De Gregorio et al., 2021). Identifying the common neural correlates induced by psychedelic drugs may lead to a more comprehensive mechanistic understanding of therapeutic benefits. Our study informs this neurobiology.

There are numerous limitations to this investigation. First, fMRI datasets were derived from different study protocols and institutions, leading to heterogeneity (for more details, see Tables S7 and S8). LSD data were accessed from an open-resource database, in which only preprocessed data were shared (i.e., raw data were not available); the processing pipeline was distinct from the other datasets. Second, 3T resolution precludes the ability to make meaningful inferences regarding psychedelic effects on subcortical structures, such as those in the brainstem. Third, nitrous oxide was the only drug formally and prospectively studied for psychedelic phenomenology; volunteers participating in the secondary datasets did not have the same assessment. Thus, we must be circumspect in comparing the psychedelic experience across these drug protocols and restrict interpretation to the neural correlates of psychedelic drug administration. Fourth, although both nitrous oxide and ketamine are thought to act at NMDA receptors, there are other distinct targets considered critical for sedative-hypnotic effects, e.g., HCN1 channels for ketamine (Chen et al., 2009). Thus, it is not clear what accounts for the changes in subjective experience. Also, nitrous oxide, ketamine, and LSD were administered in different protocols to participants of different ages, without the goal of achieving a consistent target state. This also limits inferences that can be drawn about commonalities across the three drugs. Although we found that nitrous oxide, ketamine, and LSD all reduced within-network functional connectivity and increased between-network connectivity, including shared effects on TPJ and IPS connectivity, we did not statistically demonstrate the precise similarity of these network reconfigurations; further studies need to be performed. Finally, additional psychedelic drugs such as psilocybin, dimethyltryptamine, and methylenedioxymethamphetamine should be investigated for their effects on connectivity in the posterior cortical hot zone.

Despite these limitations, this study is the first to characterize functional connectivity changes during the administration of psychedelic doses of nitrous oxide and, to our knowledge, the first study to identify cortical network reconfigurations that appear common to the administration of both classical and non-classical psychedelic drugs. Finally, these network alterations occur consistently in a posterior cortical region argued to be critical for the content of consciousness (Koch et al., 2016), presenting a neurobiologically plausible set of network nodes that mediate the psychedelic experience.

Data and code availability statement

Publicly available software used for analyses is CONN toolbox (https://web.conn-toolbox.org/). All data needed to evaluate the conclusions in this article are present in the main text and the Supplementary Materials. Access to additional data (nitrous oxide, ketamine, and propofol) by qualified investigators (i.e., affiliated with accredited academic and research institutions) are subject to scientific and ethical review. Completion of a material transfer agreement signed by an institutional official will be required in order to access the data. The LSD dataset is published at Openneuro (doi:10.18112/openneuro.ds003059.v1.0.0)

Ethics statement

This study was conducted at the University of Michigan Medical School, where Institutional Review Board (IRB, HUM00096321) approval was obtained. The study team carefully discussed risks and benefits with all participants, after which written informed consent was documented. This analysis was part of a clinical study registered with clinicaltrials.gov (NCT03435055); results from the primary study were posted in July 2021. All methods were performed in accordance with the relevant guidelines and regulations and written informed consent was obtained.

Declaration of Competing Interest

The authors have no conflicts of interest to declare.

Credit authorship contribution statement

Rui Dai: Conceptualization, Methodology, Visualization, Writing – original draft, Writing – review & editing. **Tony E. Larkin:** Investigation, Writing – review & editing. **Zirui Huang:** Conceptualization, Methodology, Visualization, Writing – original draft, Writing – review & editing. **Vijay Tarnal:** Investigation, Writing – review & editing. **Paul Picton:** Investigation, Writing – review & editing. **Phillip E. Vlisides:** Investigation, Writing – review & editing. **Ellen Janke:** Investigation, Writing – review & editing. **Amy McKinney:** Investigation, Writing – review & editing. **Anthony G. Hudetz:** Methodology, Writing – review & editing. **Richard E. Harris:** Conceptualization, Methodology, Investigation, Writing – review & editing. **George A. Mashour:** Conceptualization, Methodology, Investigation, Supervision, Writing – original draft, Writing – review & editing.

Data availability

Data needed to evaluate the conclusions in this article are present in the main text and the Supplementary Materials. The LSD dataset is available at Openneuro (doi:10.18112/openneuro.ds003059.v1.0.0).

Funding

This work was funded by National Institutes of Health (Bethesda, Maryland, USA) grants R01-GM111293 (to G.A.M., R.E.H.) and T32-GM103730 (to G.A.M., PI, and Z.H., Fellow).

Supplementary materials

Supplementary material associated with this article can be found, in the online version, at doi:10.1016/j.neuroimage.2023.120097.

References

Arzy, S., Thut, G., Mohr, C., Michel, C.M., Blanke, O., 2006. Neural basis of embodiment: distinct contributions of temporoparietal junction and extrastriate body area. J. Neurosci. 26, 8074–8081. doi:10.1523/JNEUROSCI.0745-06.2006.

Berman, R.M., Cappiello, A., Anand, A., Oren, D.A., Heninger, G.R., Charney, D.S., Krystal, J.H., 2000. Antidepressant effects of ketamine in depressed patients. Biol. Psychiatry 47, 351–354. doi:10.1016/S0006-3223(99)00230-9.

Block, R.I., Ghoneim, M.M., Kumar, V., Pathak, D., 1990. Psychedelic effects of a subanesthetic concentration of nitrous oxide. Anesth. Prog. 37, 271–276.

Carhart-Harris, R.L., Muthukumaraswamy, S., Roseman, L., Kaelen, M., Droog, W., Murphy, K., Tagliazucchi, E., Schenberg, E.E., Nest, T., Orban, C., Leech, R., Williams, L.T., Williams, T.M., Bolstridge, M., Sessa, B., McGonigle, J., Sereno, M.I., Nichols, D., Hellyer, P.J., Hobden, P., Evans, J., Singh, K.D., Wise, R.G., Curran, H.V., Feilding, A., Nutt, D.J., 2016. Neural correlates of the LSD experience revealed by multimodal neuroimaging. Proc. Natl. Acad. Sci. U. S. A. 113, 4853–4858. doi:10.1073/pnas.1518377113.

Chen, X., Shu, S., Bayliss, D.A., 2009. HCN1 channel subunits are a molecular substrate for hypnotic actions of ketamine. J. Neurosci. 29, 600–609. doi:10.1523/JNEUROSCI.3481-08.2009.

Chumbley, J., Worsley, K., Flandin, G., Friston, K., 2010. Topological FDR for neuroimaging. Neuroimage 49, 3057–3064. doi:10.1016/j.neuroimage.2009.10.090.

Dashdorj, N., Corrie, K., Napolitano, A., Petersen, E., Mahajan, R.P., Auer, D.P., 2013. Effects of subanesthetic dose of nitrous oxide on cerebral blood flow and metabolism: a multimodal magnetic resonance imaging study in healthy volunteers. Anesthesiology 118, 577–586. doi:10.1097/ALN.0b013e3182800d58.

De Gregorio, D., Aguilar-Valles, A., Preller, K.H., Heifets, B.D., Hibicke, M., Mitchell, J., Gobbi, G., 2021. Hallucinogens in Mental Health: preclinical and Clinical Studies on LSD, Psilocybin, MDMA, and Ketamine. J. Neurosci. 41, 891–900. doi:10.1523/JNEUROSCI.1659-20.2020.

Foster, B.L., Liley, D.T.J., 2013. Effects of nitrous oxide sedation on resting electroencephalogram topography. Clin. Neurophysiol. 124, 417–423. doi:10.1016/j.clinph.2012.08.007.

Hemmings, H.C., Riegelhaupt, P.M., Kelz, M.B., Solt, K., Eckenhoff, R.G., Orser, B.A., Goldstein, P.A., 2019. Towards a comprehensive understanding of anesthetic mechanisms of action: a decade of discovery. Trends Pharmacol. Sci. 40, 464–481. doi:10.1016/j.tips.2019.05.001.

Huang, Z., Liu, X., Mashour, G.A., Hudetz, A.G., 2018a. Timescales of intrinsic BOLD signal dynamics and functional connectivity in pharmacologic and neuropathologic states of unconsciousness. J. Neurosci. 38, 2304–2317. doi:10.1523/JNEUROSCI.2545-17.2018.

Huang, Z., Zhang, J., Wu, J., Mashour, G.A., Hudetz, A.G., 2020. Temporal circuit of macroscale dynamic brain activity supports human consciousness. Sci. Adv. 6, 1–14. doi:10.1126/sciadv.aaz0087.

Huang, Z., Zhang, J.J., Wu, J., Qin, P., Wu, X., Wang, Z., Dai, R., Li, Y., Liang, W., Mao, Y., Yang, Z., Zhang, J.J., Wolff, A., Northoff, G., 2016. Decoupled temporal variability and signal synchronization of spontaneous brain activity in loss of consciousness: an fMRI study in anesthesia. Neuroimage 124, 693–703. doi:10.1016/j.neuroimage.2015.08.062.

Huang, Z., Zhang, Jun, Wu, J., Liu, X., Xu, J., Zhang, Jianfeng, Qin, P., Dai, R., Yang, Z., Mao, Y., Hudetz, A.G., Northoff, G., 2018b. Disrupted neural variability during propofol-induced sedation and unconsciousness. Hum. Brain Mapp. 39, 4533–4544. doi:10.1002/hbm.24304.

Jafri, M.J., Pearlson, G.D., Stevens, M., Calhoun, V.D., 2008. A method for functional network connectivity among spatially independent resting-state components in schizophrenia. Neuroimage 39, 1666–1681. doi:10.1016/j.neuroimage.2007.11.001.

James, W., 1874. Review of "The Anaesthetic Revelation and the Gist of Philosophy". Atl. Mon. 33, 627–628.

Jevtović-Todorović, V., Todorović, S.M., Mennerick, S., Powell, S., Dikranian, K., Benshoff, N., Zorumski, C.F., Olney, J.W., 1998. Nitrous oxide (laughing gas) is an NMDA antagonist, neuroprotectant and neurotoxin. Nat. Med. 4, 460–463. doi:10.1038/nm0498-460.

John, E.R., Prichep, L.S., Kox, W., Valdés-Sosa, P., Bosch-Bayard, J., Aubert, E., Tom, M., di Michele, F., Gugino, L.D., DiMichele, F., 2001. Invariant reversible QEEG effects of anesthetics. Conscious. Cogn. 10, 165–183. doi:10.1006/ccog.2001.0507.

Koch, C., Massimini, M., Boly, M., Tononi, G., 2016. Neural correlates of consciousness: progress and problems. Nat. Rev. Neurosci. 17, 307–321. doi:10.1038/nrn.2016.22.

Li, D., Mashour, G.A., 2019. Cortical dynamics during psychedelic and anesthetized states induced by ketamine. Neuroimage 196, 32–40. doi:10.1016/j.neuroimage.2019.03.076.

Li, D., Vlisides, P.E., Mashour, G.A., 2022. Dynamic reconfiguration of frequency-specific cortical coactivation patterns during psychedelic and anesthetized states induced by ketamine. Neuroimage 249, 118891. doi:10.1016/j.neuroimage.2022.118891.

Liechti, M.E., Dolder, P.C., Schmid, Y., 2017. Alterations of consciousness and mystical-type experiences after acute LSD in humans. Psychopharmacology 234, 1499–1510. doi:10.1007/s00213-016-4453-0, (Berl).

Mars, R.B., Sallet, J., Schüffelgen, U., Jbabdi, S., Toni, I., Rushworth, M.F.S., 2012. Connectivity-based subdivisions of the human right "temporoparietal junction area": evidence for different areas participating in different cortical networks. Cereb. Cortex 22, 1894–1903. doi:10.1093/cercor/bhr268.

Nagele, P., Duma, A., Kopec, M., Gebara, M.A., Parsoei, A., Walker, M., Janski, A., Panagopoulos, V.N., Cristancho, P., Miller, J.P., Zorumski, C.F., Conway, C.R., 2015. Nitrous oxide for treatment-resistant major depression: a proof-of-concept trial. Biol. Psychiatry 78, 10–18. doi:10.1016/j.biopsych.2014.11.016.

Nagele, P., Palanca, B.J., Gott, B., Brown, F., Barnes, L., Nguyen, T., Xiong, W., Salloum, N.C., Espejo, G.D., Lessov-Schlaggar, C.N., Jain, N., Cheng, W.W.L., Komen, H., Yee, B., Bolzenius, J.D., Janski, A., Gibbons, R., Zorumski, C.F., Conway, C.R., 2021. A phase 2 trial of inhaled nitrous oxide for treatment-resistant major depression. Sci. Transl. Med. 13, 1376. doi:10.1126/scitranslmed.abe1376.

Pavone, K.J., Akeju, O., Sampson, A.L., Ling, K., Purdon, P.L., Brown, E.N., 2016. Nitrous oxide-induced slow and delta oscillations. Clin. Neurophysiol. 127, 556–564. doi:10.1016/j.clinph.2015.06.001.

Pelentritou, A., Kuhlmann, L., Cormack, J., Mcguigan, S., Woods, W., Muthukumaraswamy, S., Liley, D., 2020. Source-level cortical power changes for xenon and Nitrous oxide-induced reductions in consciousness in healthy male volunteers. Anesthesiology 132, 1017–1033. doi:10.1097/ALN.0000000000003169.

Phoumthipphavong, V., Barthas, F., Hassett, S., Kwan, A.C., 2016. Longitudinal effects of ketamine on dendritic architecture *in vivo* in the mouse medial frontal cortex. eNeuro 3. doi:10.1523/ENEURO.0133-15.2016, ENEURO.0133-15.2016.

Ryu, J.H., Kim, P.J., Kim, H.G., Koo, Y.S., Shin, T.J., 2017. Investigating the effects of nitrous oxide sedation on frontal-parietal interactions. Neurosci. Lett. 651, 9–15. doi:10.1016/j.neulet.2017.04.036.

Schartner, M.M., Carhart-Harris, R.L., Barrett, A.B., Seth, A.K., Muthukumaraswamy, S.D., 2017. Increased spontaneous MEG signal diversity for psychoactive doses of ketamine, LSD and psilocybin. Sci. Rep. 7, 46421. doi:10.1038/srep46421.

Shaffer, J.P., 1995. Multiple hypothesis testing. Annu. Rev. Psychol. 46, 561–584. doi:10.1146/ANNUREV.PS.46.020195.003021.

Studerus, E., Gamma, A., Vollenweider, F.X., 2010. Psychometric evaluation of the altered states of consciousness rating scale (OAV). PLoS ONE 5, e12412. doi:10.1371/JOURNAL.PONE.0012412.

Vlisides, P.E., Bel-Bahar, T., Nelson, A., Chilton, K., Smith, E., Janke, E., Tarnal, V., Picton, P., Harris, R.E., Mashour, G.A., 2018. Subanaesthetic ketamine and altered states of consciousness in humans. Br. J. Anaesth. 121, 249–259. doi:10.1016/j.bja.2018.03.011.

Vrijdag, X.C.E., van Waart, H., Mitchell, S.J., Sleigh, J.W., 2021. An electroencephalogram metric of temporal complexity tracks psychometric impairment caused by low-dose nitrous oxide. Anesthesiology 134, 202–218. doi:10.1097/ALN.0000000000003628.

Whitfield-Gabrieli, S., Nieto-Castanon, A., 2012. Conn: a functional connectivity toolbox for correlated and anticorrelated brain networks. Brain Connect. 2, 125–141. doi:10.1089/brain.2012.0073.

Worsley, K.J., Marrett, S., Neelin, P., Vandal, A.C., Friston, K.J., Evans, A.C., 1996. A unified statistical approach for determining significant signals in images of cerebral activation. Hum. Brain Mapp. 4, 58–73. doi:10.1002/(SICI)1097-0193(1996)4:1<58::AID-HBM4>3.0.CO;2-O.